Compressed Sensing Method for Health Monitoring of Pipelines Based on Guided Wave Inspection

Zhe Wang, Songling Huang, *Senior Member, IEEE,* Shen Wang, Shuangyong Zhuang, Qing Wang, *Senior Member, IEEE,* and Wei Zhao

Abstract—The pipeline in-service needs to be inspected in certain period to master its structural health status. Ultrasonic guided wave which can propagate along pipelines with less energy loss provides an efficient method for long-term in situ inspection. Guided wave can detect both corrosion and cracks existing in structures. To overcome the problem of huge amounts of data and to maintain defect identification accuracy, the compressed sensing method for guided wave inspection is proposed. The compression process is essentially a scheme of analog to information conversion to compress the signal. It is accomplished by random demodulation and the equivalent sampling rate below the Nyquist rate helps to save most of storage. The compressed data is recovered to the sparse spatial domain based on the constructed dictionary from a guided wave propagation model. To verify the effectiveness of proposed method, both numerical simulations and experimental investigations are conducted. The results indicate the availability of compression and high accuracy of defect location after recovery. The influences of different compression schemes and compression ratios are further analyzed. In addition, the comparisons with direct recovery without compression and traditional analysis methods demonstrate the advantageous performance of the proposed method.

Index Terms—Compressed sensing, guided wave, orthogonal matching pursuit, pipeline inspection, structural health monitoring.

I. INTRODUCTION

THE pipeline which transports oil and gas faces corrosion and stress problems in the in-service process. Damage occurs inevitably and this shortens the life span of pipelines. Ultrasonic guided wave provides a potential method for pipeline health monitoring [1]–[3]. The monitoring scheme using sensors in situ can inspect pipelines in the long term. It also helps to diagnose damage severity and predict the health status [4]–[6].

Guided wave can propagate through the thickness of pipeline over long distances, which enables detection of both surface and internal defects. Guided wave is one type of mechanical waves and it will interact with defects leading to reflected echo. Through analyzing the received echo signal, the defect information can be extracted. For pipeline inspection, circuits for excitation and reception by ultrasonic transducers had been developed and they can be used to detect corrosion and fouling [7]. Further, the multifrequency excitation pulse signal had been applied to improve the accuracy of defect location and identify adjacent defects [8]. However, guided wave has the multimodal and dispersive natures, which increase the difficulties of guided wave application. Signal post-processing methods are required to accomplish the interpretation of information in guided wave.

Analysis methods in time and frequency domain have provided useful tools to deal with guided wave signals [9]. The Hilbert Transform (HT) was applied to extract characteristics of guided wave for the purpose of damage identification [10]. Mode decomposition techniques employing chirplet transform had been introduced to separate the individual modes from received signal [11]. The Cross-Wigner-Ville distribution had been employed to separate temporally overlapped signals in the time-frequency domain and each signal component could be reconstructed using an inverse transformation [12]. The wavelet transform was adopted to extract the time of reflected signal and this method was robust in noisy environment [13]. In addition, a multiple-input multiple-output wavelet network was proposed to detect damage location and severity [14]. Time-frequency representations (TFRs) possess high accuracy in the extraction of defect information. However, when facing long-term and long-distance pipeline health monitoring, TFRs are no longer suitable due to huge amounts of data.

Recently compressed sensing (CS) was introduced and it had attracted extensive attention [15], [16]. CS could compress the signal by a scheme of analog to information conversion and recover the signal in sparse domain. The sparsity in warped frequency domain was utilized to reconstruct ultrasonic signal [17], [18]. CS had the potential as the alternative to data compression and it had been investigated for accelerometer signals and structural response signals [19]–[21]. Because guided wave could be modeled as the convolution of incident signal and reflection sequence, an adaptive sparse deconvolution method was proposed to distinguish overlapped wavepackets [22]. However, the recovery or reconstruction attracts more attention in guided wave field. In the health monitoring of pipelines, huge amounts of inspection data is inevitable and the process of compression is crucial in actual system.

Z. Wang, S. Huang, S. Wang, S. Zhuang and W. Zhao are with the State Key Laboratory of Power System, Department of Electrical Engineering, Tsinghua University, Beijing 100084, China (e-mail: huangsling@mail.tsinghua.edu.cn).

Q. Wang is with the Department of Engineering, Durham University, Durham DH1 3LE, U.K.

In the work described here, compressed sensing method for long-term guided wave inspection is proposed. It includes the compression and recovery processes. The pipeline inspection is conducted in regular periods. After the compression by random demodulation, the equivalent sampling rate is below the Nyquist rate and only a small proportion of data is stored in flash disk. Then a dictionary based on propagation theory is designed and the compressed data is recovered in spatial domain. The health status of pipelines is determined by analyzing the variation trend of sparse coefficients. The main contributions of this work are as follows: (1) Propose the complete compression and recovery scheme for reliable guided wave inspection. (2) Compare data compression performances of different compression methods. (3) Successfully recover the sparse coefficients containing the defect information. (4) Detect and localize the defect with high accuracy with the use of CS.

The research is organized as follows. Section II provides related work to this research. Section III presents the characteristic analysis of guided wave. In section IV, the compressed sensing method for long-term inspection is proposed and its procedures are described in detail. The validation of the proposed method is conducted firstly through simulation analysis in Section V. Section VI implements the experimental investigations and compares the method with the process of direct recovery and traditional guided wave analysis method. Concluding remarks are given in Section VII.

II. RELATED WORK

After the proposal of CS, its contents have been extensively investigated in structural health monitoring. Ultrasonic signals in plate were considered as a pulse stream model and projected in sparse warped frequency domain. This method used the CS algorithm to estimate the wave path length in a high precision [17]. The wavelet packet transform and frequency warping were combined to accomplish the sparse decomposition of dispersive guided wave based on Best-Basis theory [18]. Further, by exploiting the sparsity of wavefield in different domains, acoustic wavefield data was recovered and the damages were imaged for plate structure [23], [24].

The aspect of data compression of CS was investigated for accelerometer signals from bridge [19]. The compression ratios were limited because the data was not naturally sparse in the Fourier basis and wavelet basis. A non-uniform lowrate random sensing framework based on CS was explored for structural response signals and the modal identification could be accomplished after the recovery [20]. Structural response data of reinforced concrete was compressed by exploiting the sparsity in the wavelet basis. Due to the reduced data sampling, CS could help to reduce the energy and storage costs in wireless sensor networks [21]. However, the analysis and discussion of CS, especially the compression process, are still inefficient.

Sparse recovery which utilizes the sparsity of signal is adopted to deal with guided wave. Exploiting the sparsity of structural damage, Lamb wave signal was decomposed by the sparse reconstruction technique based on basis pursuit denoising and matching pursuit [25]. Similarly, the sparse reconstruction approach was able to localize multiple acoustic

emission events occuring closely in time [26]. For characterizing pipeline defects, an optimized dictionary was designed and sparse representation with dispersion based matching pursuit was developed [27], [28]. This method can deal with overlapped dispersive wave-packets. Further, the dictionary atom design and dictionary learning were employed to better
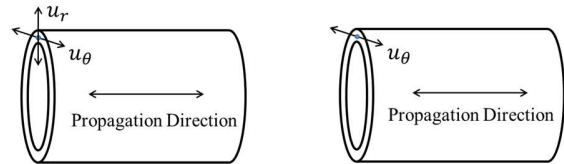

Fig. 1: Wave propagating along the axial direction in pipe. The left is longitudinal mode and the right is torsional mode.

solve the sparse reconstruction in guided wave detection [29], [30].

In addition to CS, other techniques in data science and engineering also attract attention in the field of structural health monitoring [31]. A novel framework called DeepSHM was presented to classify damage using deep learning (DL) [32]. It trained the neural weights by wavelet coefficient matrix and extracted feature patterns. Computer vision and deep learning were combined to analyze acceleration data [33]. It trained a deep neural network (DNN) for anomaly classification from large amounts of data. Besides, machine-learning based condition assessment had been developed for monitoring girders and stay cables [34], [35]. This approach extracted the features and analyzed the patterns to determine the structural status. Deep learning and machine learning provides new perspectives which are different from CS. However, deep learning requires prior knowledge and data set to train the network. Machine learning is advantageous to identify the modal response, but it is still a post-processing method to analyze the signal sampled under Shannon's theorem. In contrast to this two schemes, compressed sensing can compress data in the sampling process and then decrease the data volume to transfer.

III. CHARACTERISTIC ANALYSIS OF GUIDED WAVE

Through solving the elastodynamic equation combined with boundary conditions, the characteristic equation of guided wave can be obtained [36], [37]. Three types of guided wave exist in a hollow cylinder structure: longitudinal (L(0,m)), torsional (T(0,m)) and flexural (F(n,m)) mode. The integers n and m denote the circumferential order and group order of one mode respectively.

The three modes have different vibration characteristics. L and T mode are commonly used modes and they are shown in Fig. 1. u_r, and u_θ represent the radial and circumferential displacement, respectively. T mode is simple and it has only one displacement component along the circumferential direction. The in-service pipeline might be buried underground or covered by an insulation layer. Guided wave propagating along the pipeline will interact with the outer environment and this leads

to energy leakage. Due to the circumferential displacement direction, T mode has less energy loss than the other two modes.

The characteristic equations of guided wave can be solved by numerical method. For steel material with Young's modulus of 207 GPa, Poisson's ratio of 0.3 and mass density of 7800 kg · m^{-3}, the results are shown in Fig. 2. The curves describe the relation between wave velocity and frequency. Guided waves of different frequencies have different velocities, which
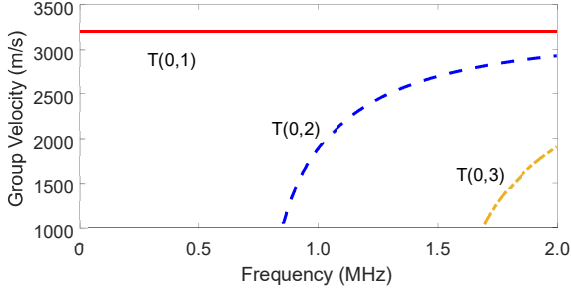

Fig. 2: Dispersion curve for guided wave of torsional mode. The group velocity varies as a function of frequency.

is a typical feature. This phenomenon is called dispersion [38]. It is nearly impossible to generate pure single-frequency signal of limited time duration. Therefore, the excitation signal usually owns a certain bandwidth. With the long propagation distance, the dispersion will bring the elongation of wavepackets and lead to difficult interpretation in post-processing.

To overcome the negative effect of dispersion, T(0,1) is chosen as the inspection guided wave because its velocity does not vary with frequency.

The propagation model of guided wave can be analyzed in theoretical expression [39]. The out-of-plane surface displacement of guided wave can be denoted as $u(x,t)$, where x is the propagation distance and t is the time. The input signal to the transducer is $f(t)$ and it means at the location of transducer $u(0,t) = f(t)$. According to the propagation of guided wave, the displacement of any point in time and space can be calculated by the phase shift of excitation signal:

$$u(x,t) = \int_{-\infty}^{\infty} F(\omega)e^{i(k(\omega)x - \omega t)}d\omega \tag{1}$$

where ω is the angular frequency, $F(\omega)$ is Fourier transform of $f(t)$ and $k(\omega)$ is the wavenumber as a function of ω. Further, wavenumber is expressed as:

$$k(\omega) = \frac{\omega}{v_p(\omega)}. \tag{2}$$

where v_p is the phase velocity which can be derived from the dispersion relation. The received signal from the receiver is the superposition of reflection waves from discontinuities at different locations:

$$x(t) = \sum_j \int_{-\infty}^{\infty} A_j F(\omega)e^{i(k(\omega)r_j - \omega t)}d\omega \tag{3}$$

where A_j is the reflection coefficient and r_j is the round trip distance. In the inspection of pipeline, the identification of the locations and severities of reflectors are important objects.

IV. COMPRESSED SENSING METHOD FOR GUIDED WAVE

INSPECTION

In the long-term health monitoring system, the inspection data is sampled and stored every certain period. For important pipelines, the monitoring may be implemented in a real-time way. This will generate numerous data. For multiple pipelines of 10 km long, when sampling frequency of 500 kHz are
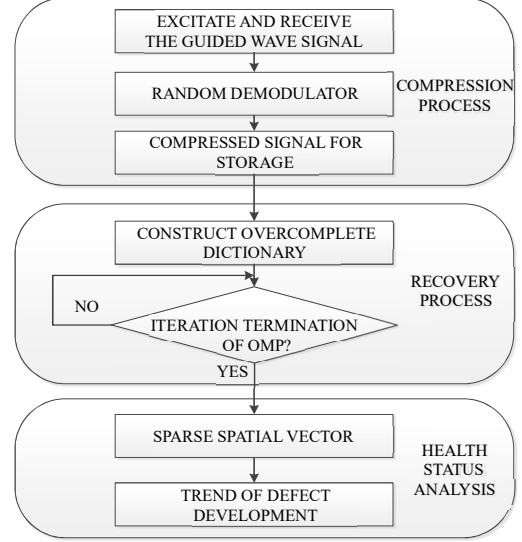

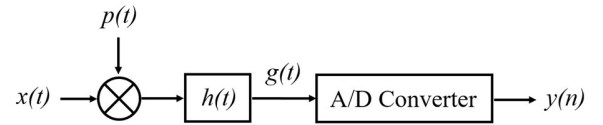Fig. 3: Schematic diagram for the compressed sensing method.

Fig. 4: Schematic diagram for the random demodulator.

used, the inspection data may reach hundreds of gigabytes. To address the storage problem and also detect the flaws accurately, the compressed method is proposed. The complete diagram of the proposed method is summarized in Fig. 3.

A. Process of Compression

To achieve the goal of sub-Nyquist sampling, several strategies have been put forward, including the random demodulator (RD), modulated wideband converter (MWC) and multi-coset sampler.

RD is a uniform sub-Nyquist sampling method [40]. Its schematic diagram is depicted in Fig. 4. This system contains three parts: demodulation, lowpass anti-aliasing filtering and low-rate analog-to-digital (A/D) converter. The input signal $x(t)$ is bandlimited and its time duration is T. The demodulation is accomplished by multiplying a pseudonoise sequence $p(t)$. In detail, $p(t)$ is a random square wave and its value is +1 or −1. The chipping rate of $p(t)$, which is defined as the fastest rate to switch between +1 and −1, should be not smaller than the twice of highest frequency of $x(t)$. The filter $h(t)$ acts as an integrator and its impulse response is a rectangular function.

$$h(t) = \begin{cases} 1, & for\ 0 < t < T/M_s \\ 0, & otherwise \end{cases} \tag{4}$$

where $T_s = T/M_s$ is the sampling period also used in the A/D conversion process. Then sampling frequency f_s is M_s/T which is usually smaller than the Nyquist rate. After the sampling procedure, the discrete signal is obtained and denoted as $y(k)$. From Fig. 4, $g(t)$ can be expressed as:

$$g(t) = x(t)p(t) * h(t) = \int_{t-\frac{T}{M_s}}^{t} x(\tau)p(\tau)d\tau \tag{5}$$

where $*$ denotes convolution. Then

$$y(k) = g((k+1)T_s) = \int_{kT_s}^{(k+1)T_s} x(\tau)p(\tau)d\tau \tag{6}$$

where $k = 0,1,\cdots,M-1$. By solving the $y(k)$, the theoretical solution can be obtained and it can be expressed in matrix form:

$$y = \Phi x \tag{7}$$

where Φ is the measurement matrix. The non-zero elements of Φ are from the pseudonoise sequence and Φ can be considered as a random matrix. x represents the physical waveform of signal received by the sensor. Through the compression, the sampling rate can be not limited by the sampling theorem and only a small proportion of discrete data is stored in y. Thus, the storage of inspection data is reduced greatly. y preserves the information of physical signal. After the process of recovery, the characteristics will be revealed.

B. Construction of Dictionary for Sparse Domain

The condition for recovery process is that the signal itself is sparse or it can be transformed to certain sparse domains.

In the case of pipeline inspection, defects such as notches are sparse in space. The received signal x can be transformed to the spatial domain by overcomplete dictionary. x is considered to be the superposition of reflected signal from multiple scatterers in pipeline. According to (3), x can be expressed as:

$$x(t) = \sum_n A_n d_n(n,t) + e_x(t) \tag{8}$$

where $d_n(n,t)$ denotes the waveform from defect and $e_x(t)$ is noise. The value A_n indicates the defect severity to some extent. Moreover, the form of linear combination can be represented in matrix multiplication:

$$x = Da + e \tag{9}$$

where D is the overcomplete dictionary of potential scattered signal, which contains $d_n(n,t)$, a is the sparse vector. The nonzero entries in a corresponding to scatters. Every column of the dictionary, which is called an atom, indicates the waveform of one defect in a certain distance. This means x can be decomposed by signal from potential defect. Therefore, the design of redundant dictionary D should be deliberate. To contain the potential defect location, the propagation distance is discreted averagely to M parts. The total reflection waveform of each part without energy loss is formed into one atom in the dictionary:

$$D = [d_1,d_2,\cdots,d_j,\cdots,d_M] \tag{10}$$

where d_j is the wavepacket reflected from different parts with different round trip distances and it can be derived from the guided wave propagation model.

The tone-burst is selected as input signal $f(t)$, which is used to excite the guided wave. The sinusoidal signal modulated by Hanning window is adopted as the tone-burst:

$$f(t) = A\left(0.5 - 0.5 \cdot \cos\frac{2\pi f_c t}{N_c}\right)\sin 2\pi f_c t \tag{11}$$

where A is the amplitude of input signal, f_c is the center frequency and N_c is the number of periodicity.

According to propagation model, the initial atoms can be obtained:

$$d_j = u(r_j,t) \qquad d_j \in D. \tag{12}$$

Actually, the attenuation will occur inevitably in the propagation of guided wave. It will lead to the reduction of wave amplitude. Different materials have different attenuation characteristics. To acquire the quantification of the attenuation, the finite element method (FEM) is adopted. The attenuation coefficient is expressed as the ratio of amplitude of reflected wave with that of the original point.

$$d_j = C_j u(r_j,t)\ d_j \in D \tag{13}$$

where C_j is attenuation coefficient. As can be seen in (9), the guided wave signal matches the form of compressed sensing. By solving the estimation of a, the location of defect, even the severity can be determined.

C. Process of Recovery

The pipeline inspection problem is to solve $\hat{a}$ which denotes the estimation of a. Combining (7) with (9), the problem is expressed as

$$y = \Phi Da + e_y = \Theta a + e_y \tag{14}$$

where y is the compressed measurement, ΦD is denoted as Θ and e_y is the noise term. D is the $N \times M$ matrix and satisfies $N \ll M$ to provide enough atoms. The problem is underdetermined and the number of solutions is infinite. The problem of (14) can be written in vector form as

$$\begin{bmatrix} y_1 \\ y_2 \\ \vdots \\ y_N \end{bmatrix} \approx \hat{a}_1 \begin{bmatrix} \Theta_{11} \\ \Theta_{21} \\ \vdots \\ \Theta_{N1} \end{bmatrix} + \hat{a}_2 \begin{bmatrix} \Theta_{12} \\ \Theta_{22} \\ \vdots \\ \Theta_{N2} \end{bmatrix} + \cdots + \hat{a}_N \begin{bmatrix} \Theta_{1M} \\ \Theta_{2M} \\ \vdots \\ \Theta_{NM} \end{bmatrix}. \tag{15}$$

Greedy algorithms and convex optimization are the two most common solving methods. The computation cost of the former one is less than that of the latter one. Orthogonal matching pursuit (OMP), one of the greedy algorithms, selects the most matched column in Θ at a time and determines the value of $\hat{a}_i$. Once a certain column is selected, it will not be considered in the following iteration. This is in accord with the defect location identification problem. If one defect location is found out, then the object is to find next location. OMP can be expressed as:

$$\min \|\hat{a}\|_0 \qquad s.t.\ \|\Theta\hat{a} - y\|_2 \le \varepsilon \tag{16}$$

where ε is the stopping condition and $\|\hat{a}\|_0$ is the l_0 norm term which is the number of non-zero elements in $\hat{a}$. The aim of solution is to find the sparsest vector $\hat{a}$. The flowchart of algorithm is presented in Fig. 5. In the flowchart, K is sparsity which is an integer meaning the maximum number of defect in this case.
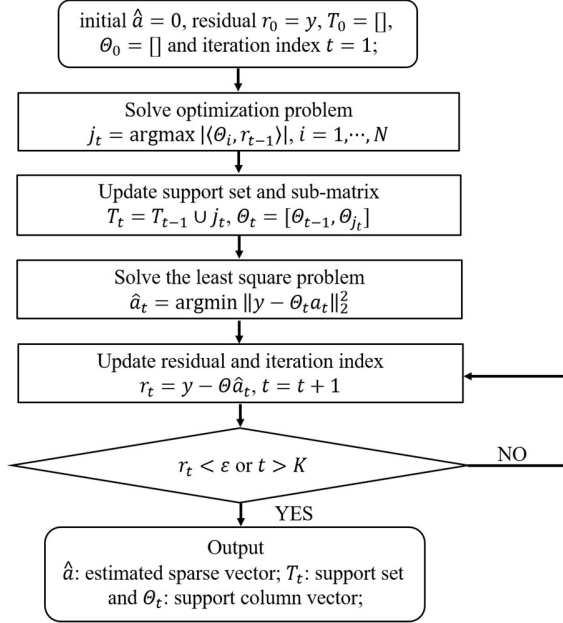

Fig. 5: The flowchart of recovery process by orthogonal matching pursuit.

D. Health Status Analysis of Pipe

After the recovery of the sparse vector, the structural health status can also be judged. When guided wave encounters the defects, a certain proportion of energy will be reflected back and the other will propagate forward. The quantitative experimental study indicates that the reflection coefficients of T(0,1) mode increase with the depths of defects to some extent [41]. Defect depth is a vital parameter because the larger depth means the thinner pipeline wall and the more dangerous situation.

Based on the recovery process, the sparse vector from multiple inspection data can be analyzed to find the variation trend along lapse of time. The positions of non-zero entries in sparse vector are corresponding to the defect locations and the values represent the characteristics of defects. To determine the health status, extraction method for defect development trend is implemented. Firstly, the threshold is set to exclude noise. When the value of non-zero entry is larger than the threshold, the situation is considered as a potential defect. Secondly, the non-zero entries of each position are extracted in sequences along the inspection period. Then the data is fitted to search for the varying trend and pattern. According to the pattern, the decision of pipeline health status is made. In the following parts, effectiveness verifications are conducted in both simulations and experiments.

V. NUMERICAL ANALYSIS

A. Simulation and Corresponding Results

The proposed compressed sensing method for guided wave inspection is firstly verified by numerical analysis. COMSOL Multiphysics (COMSOL Inc., Sweden), one commercial FEM software, is applied to simulate the propagation of T mode guided wave in pipeline and its interaction with defect.
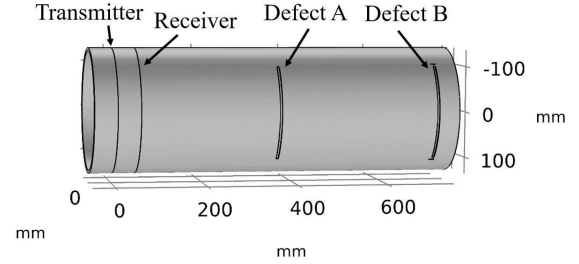

Fig. 6: The simulation model of pipeline for guided wave. Two defects are constructed on the pipeline.

The object of numerical analysis is to imitate the actual oil and gas pipeline. Therefore, the geometric shape of pipeline structure set in the software is from the size of pipeline inservice. The outer diameter and thickness of the structure are 273 mm and 6 mm respectively. And the attributes of steel are adopted as the properties of simulation material. A pressure of 5 MPa is added to the pipeline inner wall to simulate the pressure from the inner fluid. To generate T mode, circumferential load is implemented on the circular cross section of pipeline. The end surface is set as a low reflection boundary to decrease the echo wave interference.

Two slot defects (Defect A and Defect B) are considered and constructed on the outer surface of pipeline. The model is presented in Fig. 6. The excitation load is implemented on the middle part of the pipeline, which is denoted as transmitter. The cycle number of excitation signal is 5 and the center frequency is 32 kHz. The theoretical wave velocity from dispersion relation is 3194.86 m/s. Closed to the excitation part, the receiver part is placed between the excitaion load and Defect A. The distance between the transmitter and receiver is set as 50 mm.

To obtain accurate solutions, the size of finite element mesh is a crucial parameter. In the situation of guided wave, the maximum size should be much less than the wavelength of stimulated wave. In this work, the size is chosen and expressed as:

$$\Delta x \le \frac{\lambda}{15} \tag{17}$$

where Δx is the element size and λ is the wavelength. For the element mesh near the defects, the element is divided carefully and more intensive meshes are built. Transient analysis is utilized to acquire the signal in time domain. The time step is small enough compared with the period of guided wave.

The white Gaussian noise is added to the received signal to simulate the actual situation. The signal-to-noise ratio (SNR) is set as 25 dB. The obtained original signal without compression

is shown in Fig. 7(a). The sampling rate is 250 kHz and 170 discrete points are obtained. The data is firstly compressed applying the digital RD process. After the compression, only 34 of original points are left as the stored data. The amount of data is greatly reduced and the results are presented in Fig. 7(b). The equivalent sampling rate of compressed signal is 50 kHz, which is lower than the Nyquist rate. Then these points are used to recover defect location based on the proposed
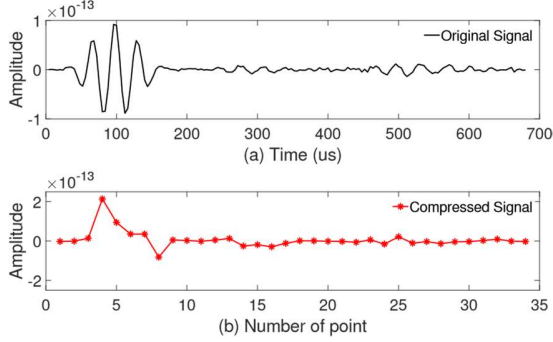

Fig. 7: The original signal from the simulation and compressed signal using the digital RD process.
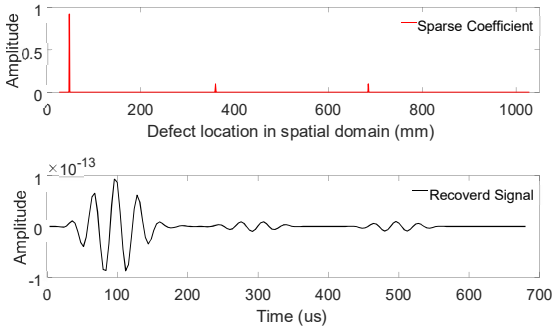

Fig. 8: The solved sparse coefficients using the OMP algorithm and the reconstructed signal.

TABLE I: Defect Location and Relative Error

Defect	Calculated Distance (mm)	Actual Distance (mm)	Relative Error
Defect A	350	368.	5	2.63%
	700	758.		
Defect B			5	2.0%

method. The solved sparse coefficients and recovered signal are shown in Fig. 8.

It can be seen that several spikes appear in Fig. 8(a). The first spike is caused by the direct wave from transmitter. The second and third spikes mean reflection waves from certain locations and potential flaws might occur. As Fig. 8(b) shows, the signal is recovered accurately. Because the added Gaussian noise cannot match the atom in the dictionary, the noise is not recovered. It indicates that the compressed sensing can filter the noise. Besides, the contained information is not lost in the compression process. To analyze the effectiveness, the relative error of the defect location estimation is calculated and shown

in Table I. The relative error is less than 3 %. It demonstrates the compressed sensing method can recover the defect location with little data. Besides, the location accuracy could meet the actual demand for defect inspection.

B. Further Analysis and Discussion

1) Comparison with other measurement matrices: For the measurement matrix Φ used in compressed sensing, full random matrices are usually adopted because of the restricted
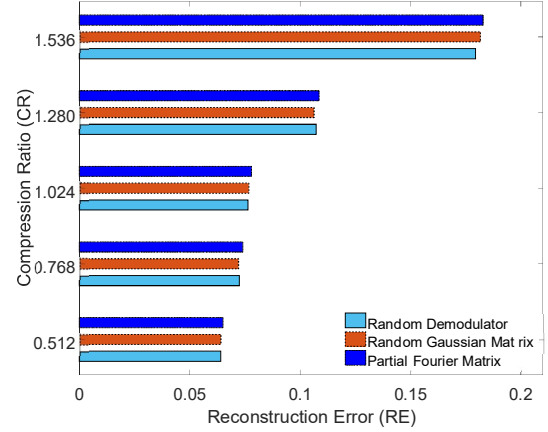

Fig. 9: The relation between compression ratio and reconstruction error.

isometry property. Probability theory is applied to construct the random matrices, including Gaussian type and Bernoulli type. Besides, structured random matrices such as partial Fourier matrices are also utilized as a measurement matrix [42]. The cases of random Gaussian matrices and partial Fourier matrices are studied in this work. It is worth noting that the implementation is accomplished in the simulation environment. However, in the actual inspection system, the sampling algorithm need to be embedded in the sensors.

The random Gaussian matrices can be formed by sampling independent and identically distributed entries from Gaussian distribution. The partial Fourier matrices are obtained from discrete Fourier matrices. To better compare the different measurement matrices, the recovery errors under different compression ratios are also investigated. The corresponding concepts and results are shown in next part where the compression ratio is studied.

2) Influence of compression ratio: In the scheme of compressed sensing, the measured and stored data is usually less than that from the sampling theorem. To analyze the data reduction, the compression ratio (CR) is calculated as

$$CR = \frac{N_o}{N_c} \qquad (18)$$

where N_o and N_c are the lengths of signal sampled under Nyquist rate and compressed signal, respectively. Further, the reconstruction error (RE) is defined as

$$\xi = \frac{\|\hat{x} - x\|_2}{\|x\|_2} \qquad (19)$$

where $\hat{x}$ is the reconstructed data from the CS. Fig. 9 shows the relation between CR and RE. The results of different measurement matrices are also presented.

The Nyquist rate, which is twice the frequency of signal is 64 kHz in this case. The larger compression ratio means the less sampling rate and the less data. From fig. 9, the RE increases with CR for different measurement matrices. Even oversampling the signal when CR is 0.512, the RE is approximately 7 %. The error is mainly brought by the
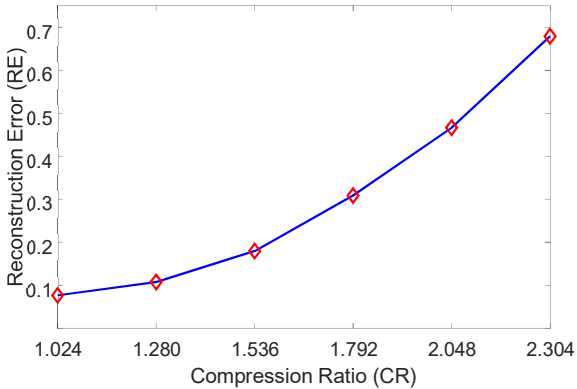

Fig. 10: The compression ratio and corresponding reconstruction error for random demodulator.

Gaussian noise and the mismatch of the dictionary with signal. The noise is difficult to recover using the dictionary and the method to reduce noise is not discussed here. The constructed dictionary can be designed more deliberately by the dictionary learning to diminish the error. For different measurement matrices, the errors have the same order of magnitude and none measurement matrix is significantly superior to the other two matrices. It indicates that the optimization of dictionary is the key point in the accurate recovery and it still needs more effort.

Furthermore, the larger CRs are studied for a random demodulator to investigate the upper limit of compression. The results are illustrated in Fig. 10. The RE increases with the CR in a non-linear way. When the CR equals to 1.792, the RE reaches 30 %. Therefore, to ensure the recovery accuracy, the CR needs to be no more than 6 and the equivalent sampling rate is 41.7 Hz. Considering the actual system uses sampling theorem, the sampling rate should be larger than the Nyquist rate, even 5 or more times of the signal frequency. Thus, the scheme of compressed sensing is advantageous in data compression.

VI. EXPERIMENTAL INVESTIGATIONS AND DISCUSSION

A. Experimental Setup

Experiments are conducted on an in-service oil pipeline which is buried underground. The system of pipeline health monitoring is depicted in Fig. 11(a). Electromagnetic acoustic transducer (EMAT) is adopted to generate T mode guided wave. EMAT is fixed on the buried pipeline to accomplish the in situ monitoring. The lead wires are connected to terminal box placed on the ground. The tone-burst with an amplitude of 50 V

is loaded on the EMAT of transmitter. The received signal is firstly amplified and filtered by signal conditioning circuits.

EMAT is composed of two parts: the iron-nickel alloy belt and coil. The photograph of buried EMAT is provided in Fig. 11(b). To avoid the negative effect of two directional waves, the principle of wave interference is utilized to generate unidirectional guided wave. Two coils with same number of turns are wrapped around the pipeline. The distance of two coils are the odd times of one quarter wavelength. The excitation signal flown into the two coils owns the same amplitude but phase difference of odd times of $\pi/2$. Then the waves are superimposed on each other side of the coils. In one direction, the waves are enhanced to double amplitude, while in another direction, the waves are offset to zero. Thus, the guided waves only propagate in one direction and the echoes can be located to find the defects.

B. Compressed Sensing Method for Defect Inspection

The inspection data is collected every week to master the situation of in-service pipeline. The data is sampled at the rate of 1 MHz, which is set up by the data acquisition (DAQ) system. The waveforms of inspection data in three weeks without compression are shown in Fig. 12. The wavepacket near the start time is the direct wave signal and electromagnetic induction signal. It is neglected in the following analysis. To apply the proposed compressed sensing method and not increase the cost of hardware when adapting to the existing guided wave inspection system, the compressed procession is accomplished numerically instead of establishing the physical RD system. After the compression, the equivalent sampling rate is 50 kHz and it is less than the Nyquist rate. Thus 95% of storage space has been saved. Then the compresssed data is stored in flash disk.
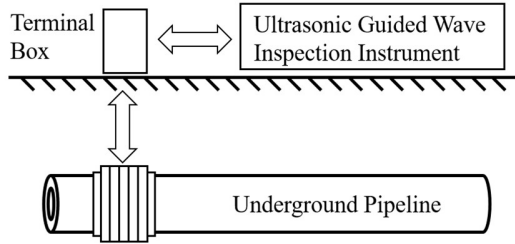
The compressed discrete points are further analyzed by the recovery method. The solved sparse coefficients are presented in Fig. 13. Several spikes appear and they vary with different weeks. It is noticed that the value in location around 0.6 m is quite large, which means the large amplitude of reflection wave. In the three inspections, the locations of maximum values are at 6.382, 6.382 and 6.324 m, respectively. The location differences are quite small.

Through observing the variation trend of the maximum coefficients of three weeks, it can be found that the values are increasing, which implies that the defect is extended with time. The pipeline is threatend by potential flaws. Then the pipeline is excavated to search for the reason of the increased reflection wave. The photo of the excavation site is presented in Fig. 14. The pit is clearly shown which might threaten the pipeline safety. Therefore, the compressed sensing method could be an alternative way to apply in the guided wave inspection.
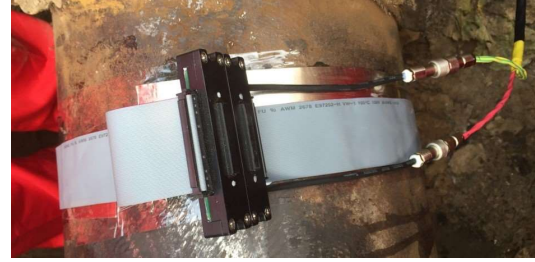
Furthermore, the distance between the actual found pit and receiver is at 6.513 m. Considering the spike location in the sparse vector, the error can be calculated and it is less than 0.2 m. The relative error is less than 3%. This demonstrates the accuracy of the compressed sensing method in terms of the defect location.

C. Comparison of Performance

1) Direct recovery without compression: The compressed sensing method utilizes few stored data to recover the sparse space vector. The reconstructed signal is close to the original signal without compression. This means the information of signal is stored in the compression process. For comparison, original signal of the third inspection week is directly recovered to space domain without compression process. The location of

to the actual defect location is a little smaller than the above compressed method, but the difference is not remarkable.

2) Existing CS method: In the theory of CS, the accurate recovery from the compressed signal is important process. Since the signal is sparse in certain domain, it can be recovered using l_0 norm term. In the above proposed method, OMP based on l_0 norm term is utilized. Besides, basis pursuit (BP) is also applied to recover the signal. The model of the BP problem can

(a) Schematic diagram for pipeline health monitoring

(b) Photo of the transducer

Fig. 11: The experimental system for underground pipeline inspection. The transducer is fixed around the pipeline and the lead maximum value appears in 6.352 m. The relative error wires are connected to a terminal box on the ground.
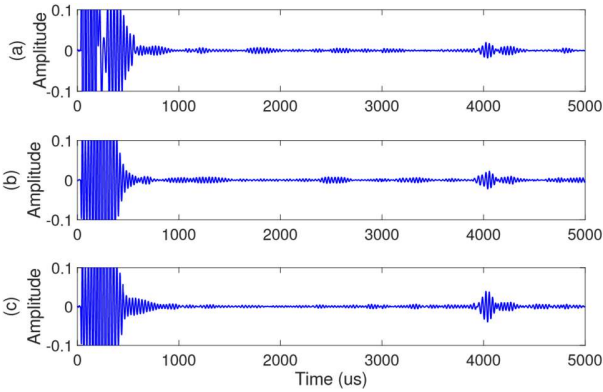
be expressed as

Fig. 12: Original waveforms of inspection data in three weeks. (a) The first week. (b) The second week. (c) The third week.
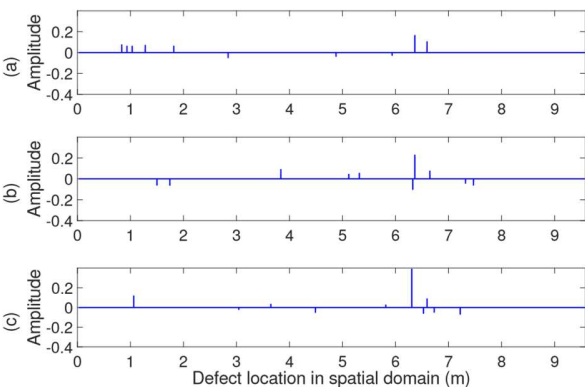

Fig. 14: The photo of found pit in pipeline.

$$\min \|\hat{a}\|_1 \qquad s.t. \ \|\Theta\hat{a} - y\|_2 \le \varepsilon \qquad (20)$$

where $\|\hat{a}\|_1$ is the l_1 norm term. The aim of BP is to search the sparsest $\hat{a}$, which is same as OMP.

The BP process is equivalent to convex optimization problem. Classic algorithms to solve (20) include BP-Simplex and BP-Interior. The former algorithm is employed in this case to compare with the effect of OMP. The inspection data from the third week in the experiment is used to calculate the RE. Under the equivalent sampling rate of 50 kHz, the RE of the BP and OMP after the recovery of signal are 7.92 % and 7.78 %, respectively. The difference of the two errors is comparatively small. Therefore, the proposed method to recover the guided wave signal is effective. Meanwhile, it indicates that the recovery process using OMP or BP has little promotion in the reconstruction accuracy. More precise analysis and model of guided wave propagating and interaction with defect will become the key to better recover the signal from compressed data.

3) Traditional analysis method: The envelope is usually extracted to analyze the signal in time domain. The signal envelope can be obtained by using the absolute value of

Fig. 13: The recovered sparse coefficients from compressed data of three weeks.

corresponding analytic signal. The analytic signal is complexvalued and it can be expressed as

$$z(t) = x(t) + j\hat{x}(t) \tag{21}$$

where $\hat{x}(t)$ is the imaginary part of analytic signal and can be obtained by Hilbert Transform. The Hilbert Transform of $x(t)$ is

$$\hat{x}(t) = x(t) * \frac{1}{\pi t} = \frac{1}{\pi} \int_{-\infty}^{+\infty} \frac{x(\tau)}{t - \tau} d\tau. \tag{22}$$
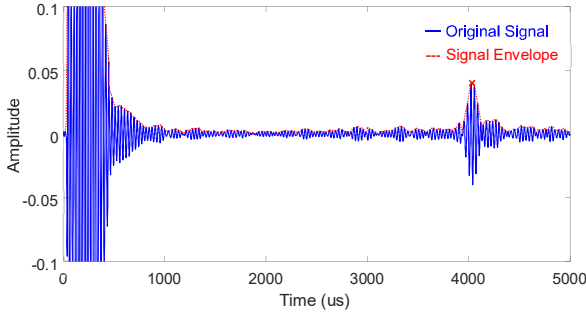

Fig. 15: The signal envelope is extracted to obtain the time information.

Then the envelope of signal can be utilized to determine the time of flight and defect location. The result of obtained envelope for the original inspection data in the third week is presented in Fig. 15.

Through the extracted times of the peak of reflection wave and the original excitation tone-burst, the time of flight is 3955 *us*. Then the defect location is 6.318 m. The error with the actual distance is 19.5 cm, which is a little larger than the compressed sensing method. However, HT is sensitive to the peak value. Noise from experimental environment might influence the accuracy. In the compressed sensing method, the spatial resolution is determined by the designed dictionary. Considering the computation cost, the columns of dictionary are limited. The accuracy of proposed method could be improved by enlarging the dictionary, which is advantageous compared with the HT method.

VII. CONCLUSION

The compressed sensing scheme is proposed for longterm pipeline inspection. Based on the thought of information sampling, the equivalent sampling rate could be not limited by the sampling theorem. Compared with the existing guided wave inspection, few data is stored and it decreases the usage of flash disk. The compression is accomplished by digital random demodulation to adapt to the present guided wave inspection instruments. For the T mode of 32 kHz in pipeline, the equivalent sampling rate is 50 kHz in this work. It is below the Nyquist rate and far less than that of actual DAQ system. After the recovery of compressed data, the sparse vector is obtained and it contains the defect location information. Both the simulations and experiments demonstrate the high accuracy of defect location. The relative error with actual defect location is less than 3 %. The analysis with different measurement matrices points out the constructed dictionary is significant to improve the recovery accuracy. Besides, the compression process has an upper limit due to the reconstruction error. The comparison with traditional locating method indicates the effectiveness of the proposed method. It is worth mentioning that the performance can be improved by designing a more deliberate dictionary. Therefore, the compressed sensing method could be a potential scheme in guided wave inspection.

REFERENCES

[1] D. Alleyne and P. Cawley, "The long range detection of corrosion in pipes using lamb waves," in *Review of progress in quantitative nondestructive evaluation*, ser. Review of progress in quantitative nondestructive evaluation. Springer, 1995, pp. 2073–2080.

[2] S. Legendre, D. Massicotte, J. Goyette, and T. K. Bose, "Neural classification of Lamb wave ultrasonic weld testing signals using wavelet coefficients," *IEEE Transactions on Instrumentation and Measurement*, vol. 50, no. 3, pp. 672–678, 2001.

[3] P. Tse, Z. Fang, and K. Ng, "Novel design of a smart and harmonized flexible printed coil sensor to enhance the ability to detect defects in pipes," *NDT & E International*, vol. 103, pp. 48–61, 2019.

[4] E. Kannan, B. W. Maxfield, and K. Balasubramaniam, "SHM of pipes using torsional waves generated by in situ magnetostrictive tapes," *Smart Materials and Structures*, vol. 16, no. 6, pp. 2505–2515, 2007.

[5] Y. Zhang, S. Huang, W. Zhao, S. Wang, and Q. Wang, "Electromagnetic ultrasonic guided wave long-term monitoring and data difference adaptive extraction method for buried oil-gas pipelines," *International Journal of Applied Electromagnetics and Mechanics*, vol. 54, no. 3, pp. 329–339, 2017.

[6] P. Aryan, A. Kotousov, C. T. Ng, and B. Cazzolato, "A model-based method for damage detection with guided waves," *Structural Control and Health Monitoring*, vol. 24, no. 3, 2017.

[7] J. D. S. J., G. W. M., D. A. F. P., and S. D. R. N. J., "Development of circuits for excitation and reception in ultrasonic transducers for generation of guided waves in hollow cylinders for fouling detection," *IEEE Transactions on Instrumentation and Measurement*, vol. 57, no. 6, pp. 1149–1153, 2008.

[8] D. Zhang, Z. Zhou, J. Sun, E. Zhang, Y. Yang, and M. Zhao, "A magnetostrictive guided-wave nondestructive testing method with multifrequency excitation pulse signal," *IEEE Transactions on Instrumentation and Measurement*, vol. 63, no. 12, pp. 3058–3066, 2014.

[9] S. Wang, S. Huang, Q. Wang, Y. Zhang, and W. Zhao, "Mode identification of broadband lamb wave signal with squeezed wavelet transform," *Applied Acoustics*, vol. 125, no. Supplement C, pp. 91–101, 2017.

[10] F. Li, H. Murayama, K. Kageyama, and I. Ohsawa, "Multiple damage assessment in composite laminates

using a doppler-effect-based fiberoptic sensor," *Measurement Science and Technology*, vol. 20, no. 11, p. 115109, 2009.

[11] C.-Y. Kim and K.-J. Park, "Mode separation and characterization of torsional guided wave signals reflected from defects using chirplet transform," *NDT & E International*, vol. 74, pp. 15–23, 2015.

[12] A. B. Zoubi, S. Kim, D. O. Adams, and V. J. Mathews, "Lamb wave mode decomposition based on Cross-Wigner-Ville distribution and its application to anomaly imaging for structural health monitoring," *IEEE Transactions on Ultrasonics, Ferroelectrics, and Frequency Control*, vol. 66, no. 5, pp. 984–997, 2019.

[13] S. Legendre, D. Massicotte, J. Goyette, and T. K. Bose, "Wavelettransform-based method of analysis for Lamb-wave ultrasonic NDE signals," *IEEE Transactions on Instrumentation and Measurement*, vol. 49, no. 3, pp. 524–530, 2000.

[14] H. Z. Hosseinabadi, B. Nazari, R. Amirfattahi, H. R. Mirdamadi, and A. R. Sadri, "Wavelet network approach for structural damage identification using guided ultrasonic waves," *IEEE Transactions on Instrumentation and Measurement*, vol. 63, no. 7, pp. 1680–1692, 2014.
[15] E. J. Candes, J. Romberg, and T. Tao, "Robust uncertainty principles: exact signal reconstruction from highly incomplete frequency information," *IEEE Transactions on Information Theory*, vol. 52, no. 2, pp. 489–509, 2006.

[16] D. L. Donoho, "Compressed sensing," *IEEE Transactions on information theory*, vol. 52, no. 4, pp. 1289–1306, 2006.

[17] A. Perelli, T. Ianni, A. Marzani, L. Marchi, and G. Masetti, "Modelbased compressive sensing for damage localization in lamb wave inspection," *IEEE Transactions on Ultrasonics, Ferroelectrics and Frequency Control*, vol. 60, no. 10, pp. 2089–2097, 2013.

[18] A. Perelli, L. De Marchi, L. Flamigni, A. Marzani, and G. Masetti, "Best basis compressive sensing of guided waves in structural health monitoring," *Digital Signal Processing*, vol. 42, pp. 35–42, 2015.

[19] J. L. Beck, "Compressive sampling for accelerometer signals in structural health monitoring," *Structural Health Monitoring*, vol. 10, no. 3, pp. 235–246, 2011.   [41]

[20] Y. Yang and S. Nagarajaiah, "Output-only modal identification by compressed sensing: Non-uniform low-rate random sampling," *Mechanical Systems and Signal Processing*, vol. 56-57, pp. 15 – 34, 2015. [42]

[21] M. Jayawardhana, X. Zhu, R. Liyanapathirana, and U. Gunawardana, "Compressive sensing for efficient health monitoring and effective damage detection of structures," *Mechanical Systems and Signal Processing*, vol. 84, pp. 414 – 430, 2017.

[22] Y. Chang, Y. Zi, J. Zhao, Z. Yang, W. He, and H. Sun, "An adaptive sparse deconvolution method for distinguishing the overlapping echoes of ultrasonic guided waves for pipeline crack inspection,"

Measurement Science and Technology, vol. 28, no. 3, p. 35002, 2017.

[23] Y. K. Esfandabadi, A. Marzani, and L. De Marchi, "Fast guided waves inspection using compressive sensing and wavenumber domain analysis," in *2017 IEEE Workshop on Environmental, Energy, and Structural Monitoring Systems (EESMS)*, July 2017, pp. 1–6.

[24] Y. Keshmiri Esfandabadi, L. De Marchi, N. Testoni, A. Marzani, and G. Masetti, "Full wavefield analysis and damage imaging through compressive sensing in lamb wave inspections," *IEEE Transactions on Ultrasonics, Ferroelectrics, and Frequency Control*, vol. 65, no. 2, pp. 269–280, 2018.

[25] R. M. Levine and J. E. Michaels, "Model-based imaging of damage with lamb waves via sparse reconstruction," *The Journal of the Acoustical Society of America*, vol. 133, no. 3, pp. 1525–1534, 2013.

[26] B. Dubuc, A. Ebrahimkhanlou, and S. Salamone, "Sparse reconstruction localization of multiple acoustic emissions in large diameter pipelines," in *Sensors and Smart Structures Technologies for Civil, Mechanical, and Aerospace Systems 2017*, vol. 10168. International Society for Optics and Photonics, 2017, p. 101682I.

[27] P. W. Tse and X. Wang, "Characterization of pipeline defect in guidedwaves based inspection through matching pursuit with the optimized dictionary," *NDT & E International*, vol. 54, pp. 171–182, 2013.

[28] J. Rostami, P. Tse, and Z. Fang, "Sparse and dispersion-based matching pursuit for minimizing the dispersion effect occurring when using guided wave for pipe inspection," *Materials*, vol. 10, no. 6, p. 622, 2017.

[29] J. Hua, L. Zeng, F. Gao, and J. Lin, "Dictionary design for lamb wave sparse decomposition," *NDT & E International*, 2019.

[30] X. Li, S. Ding, Z. Li, H. Zhao, and B. Tan, "Defect detection on thin-wall structure via dictionary learning," in *2017 IEEE International Instrumentation and Measurement Technology Conference (I2MTC)*, May 2017, pp. 1–6.

[31] Y. Bao, Z. Chen, S. Wei, Y. Xu, Z. Tang, and H. Li, "The state of the art of data science and engineering in structural health monitoring," *Engineering*, vol. 5, no. 2, pp. 234 – 242, 2019.

[32] V. Ewald, R. M. Groves, and R. Benedictus, "Deepshm: a deep learning approach for structural

health monitoring based on guided lamb wave technique," in *Sensors and Smart Structures Technologies for Civil, Mechanical, and Aerospace Systems 2019*, vol. 10970. International Society for Optics and Photonics, 2019, p. 109700H.

[33] Y. Bao, Z. Tang, H. Li, and Y. Zhang, "Computer vision and deep learning–based data anomaly detection method for structural health monitoring," *Structural Health Monitoring*, vol. 18, no. 2, pp. 401–421, 2019.

[34] S. Wei, Z. Zhang, S. Li, and H. Li, "Strain features and condition assessment of orthotropic steel deck cable-supported bridges subjected to vehicle loads by using dense FBG strain sensors," *Smart Materials and Structures*, vol. 26, no. 10, p. 104007, 2017.

[35] S. Li, S. Wei, Y. Bao, and H. Li, "Condition assessment of cables by pattern recognition of vehicle-induced cable tension ratio," *Engineering Structures*, vol. 155, pp. 1 – 15, 2018.

[36] D. C. Gazis, "Three-dimensional investigation of the propagation of waves in hollow circular cylinders. i. analytical foundation," *The Journal of the Acoustical Society of America*, vol. 31, no. 5, p. 568, 1959.

[37] D. C. Gazis, "Three-dimensional investigation of the propagation of waves in hollow circular cylinders. ii. numerical results," *The Journal of the Acoustical Society of America*, vol. 31, no. 5, p. 573, 1959.

[38] H. Kwun and K. A. Bartels, "Experimental observation of wave dispersion in cylindrical shells via time-frequency analysis," *The Journal of the Acoustical Society of America*, vol. 97, no. 6, pp. 3905–3907, 1995.

[39] P. D. Wilcox, "A rapid signal processing technique to remove the effect of dispersion from guided wave signals," *IEEE transactions on ultrasonics, ferroelectrics, and frequency control*, vol. 50, no. 4, pp. 419–427, 2003.

[40] J. A. Tropp, J. N. Laska, M. F. Duarte, J. K. Romberg, and R. G. Baraniuk, "Beyond nyquist: Efficient sampling of sparse bandlimited signals," *IEEE Transactions on Information Theory*, vol. 56, no. 1, pp. 520–544, 2010.

[41] A. Demma, P. Cawley, M. Lowe, and A. G. Roosenbrand, "The reflection of the fundamental torsional mode from ctacks and notches in pipes" *J Acoust Soc Am*, vol. 114, No.2, pp.611-25, 2003.

[42] T. T. Do, L. Gan, N. H. Nguyen, and T. D. Tran, "Fast and efficient compressive sensing using structurally random matrices," IEEE Transactions on Signal Processing, vol.60, no.1, pp.139-154, 2012.
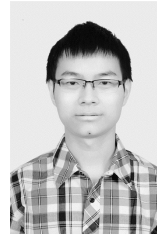
Zhe Wang received a B.S. degree from School of Electrical Engineering, Chongqing University, Chongqing, China, in 2016. He is currently pursuing a Ph.D. degree within the Department of Electrical Engineering, Tsinghua University, Beijing, China.

His current research interests include electromagnetic measurement and nondestructive evaluation.

Songling Huang received a bachelor's degree in automatic control engineering from Southeast University, Nanjing, China, in 1991, and a Ph.D. degree in nuclear application technology from Tsinghua University, Beijing, China, in 2001.

He is currently a Professor within the Department of Electrical Engineering, Tsinghua University. His research interests include nondestructive evaluation and instrument techniques.

Shen Wang received a bachelor's and Ph.D. degrees in electrical engineering from Tsinghua University, Beijing, China, in 2002 and 2008, respectively. He is currently an Associate Professor within the Department of Electrical Engineering, Tsinghua University. His research interests include nondestructive testing and evaluation, and virtual instrumentation.

Shuangyong Zhuang received a B.S. degree in measurement and instrument from Xiamen University, Xiamen, China, in 2000, and a M.S. degree in communication and information system from Sichuan University, Chengdu, China, in 2007. He is currently pursuing a Ph.D. degree with the Department of Electrical Engineering, Tsinghua University, Beijing, China.

His current research interests include modern power quality analysis.

Qing Wang received a B.Eng. in electronic instrument and measurement technique from Beihang University, Beijing, China, in 1995, a M.Sc. degree in advanced manufacturing and materials from the University of Hull, Hull, U.K., in 1998, and a Ph.D. degree in manufacturing management from De Montfort University, Leicester, U.K., in 2001.

She is currently an Associate Professor in the Department of Engineering, Durham University, Durham, U.K. Her research interests include electronic instruments and measurement, computer sim- ulation, and advanced manufacturing technology.
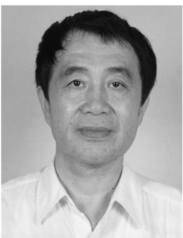
Wei Zhao received a bachelor's degree in electrical engineering from Tsinghua University, Beijing, China, in 1982, and a Ph.D. degree from the Moscow Power Engineering Institute Technical University, Moscow, Russia, in 1991.

He is currently a Professor within the Department of Electrical Engineering, Tsinghua University. His research interests include modern electromagnetic measurement and instrument techniques.